LUPINE PUBLISHERS

Open Access Journal of Biomedical Engineering and Biosciences

DOI: 10.32474/OAJBEB.2019.03.000171

ISSN: 2637-4579

Research Article

LQR-Based Design and Implementation of Lower Limb Exoskeleton Control for Paraplegic

Louay Chachati[1] and Avin Hasan[2]*

[1]*Department of Electronic Engineering, Faculty of Electrical & Electronic Engineering, University of Aleppo, Syria*

[2]*Department of Electronic Engineering/Medical Electronic Faculty of Electrical & Electronic Engineering, University of Aleppo, Syria*

***Corresponding author:** Avin Hasan, BSc, MSc, PhD (student), Department of Electronic Engineering/Medical Electronic Faculty of Electrical & Electronic Engineering, University of Aleppo, Syria

Received: October 24, 2019 **Published:** November 21, 2019

Abstract

The present paper is oriented to individuals with paraplegia as a result of spinal cord injury (SCI) and lost motion mobility. The aim of this research is to retrieve some degree of legged mobility to those people. The paper investigates the development of kinematic and dynamic models for the leg. Modeling and simulation of the system under investigation is implemented and evaluated using MATLAB/SIMULINK®. Practical results obtained from the developed lower limb model are compared with their counter parts of normal gait pattern. It is shown that the obtained results have validated the proposed approach. Both practical and simulation results have demonstrated the stability of the proposed control approach. It is believed that the proposed approach will help to establish an integrated system which emulates as accurately as possible the normal gait of human.

Keywords: Robotics; kinematic; gait pattern; LQR; PID

Introduction

Spinal cord injuries are defined by an injury to the spinal cord, which results in impairment of communication between the brain and another part of the body, which is due to an injury to the nerves in the spinal column. Signals and impulses travel from the brain, down the spinal cord, to nerves that extend throughout the body and the extremities. They also carry signals from various parts of the body, including organs, to the brain. When the spinal cord is damaged, signals can no longer travel to and from the brain, which produces pain and loss of mobility. Because of the injury, the person's brain and/or spinal cord is unable to send neuro-messages that control muscle movements or that communicate or respond to heat, cold, pressure, and pain [1]. These injuries are classified based on the level of injury, as shown in Figure1.

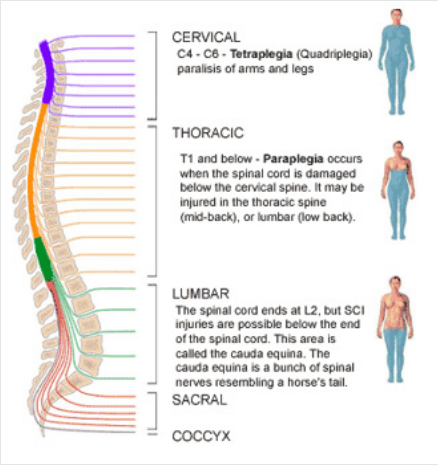

Figure 1: A single leg with relative coordinates for each joint [1].

One is exposed to paraplegia, a condition existing around us, which is define as a spinal cord injury (SCI) that paralysis the lower limbs. It is a result of severe damage to the spinal cord and the nervous system. Paraplegia mainly affects the trunk, legs, and the pelvic region, resulting in loss of movement. Many people around the world suffer from civil war, violence or because of accidents; they got hurt and unfortunately became paralyzed due to SCI or amputation one of their limbs. As mentioned, one of the most remarkable effects resulting from paralysis is the loss of mobility. Besides loss of sensory and motor function, loss of autonomic function due to SCI is followed by disturbance of heart function, blood pressure regulation, bladder function, bowel function, and patients face a great troublesomeness and a limited participation in their daily lives. Recently, in an attempt to improve the devices that help paraplegic patients to walk once again, many robotic platforms have been developed and described in literature [2]. The following up to date research focuses on exoskeletons developed specially for restore some degree of mobility in paraplegic persons. Powered lower limb exoskeletons are wearable robots attached to subject's limbs, in order to enhance their movements. They should be compliant with the user's movements and deliver at least part of the power necessary to accomplish the movements.

The primary orientation of exoskeleton research has focused on medical applications such as rehabilitation of major trauma patients and supporting mobility of spinal cord injured people (SCI). Medical exoskeletons are medical electrical equipment, which is used to provide mobility to physically disabled, injured or weak people, who are unable to walk due to a variety of medical reasons such as a SCI, neurological disorders, major trauma like stroke, cerebral palsy and so on. Recently, new strategies have also started to receive attention for presenting assistance to elderly people for doing their daily activities. With age, elderly naturally become weaker and falling becomes a worry with every step and need care and support, so there is growing urgency for such assistive technologies to help elderly people remain independent. Some researchers are trying to take preventive action with powered exoskeletons-braces for the legs with motorized joints that assist while walking. As mentioned, the field of exoskeletons are classified into non-medical and medical ones that are descried in detail in [3] and can be summarized as shown in Figure 2.

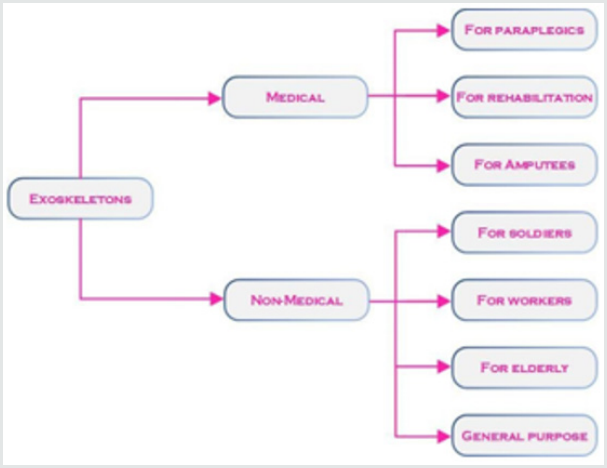

Figure 2: Classification of exoskeletons [3].

Nowadays, some active exoskeletons like the ReWalk powered orthosis has DC actuators at knee and hip joints, it consists of Dc motor for each joint, a computer and sensors. The device is powered by rechargeable batteries intended for all-day use and overnight charging, but ReWalk doesn't have balance control strategy, however the user can use [4]. Legs (Exoskeleton Lower Extremity Gait System) from Ekso Bionics and other research devices like Mina [5]. Vanderbilt exoskeleton [6] is designed to provide gait assistance to people with paraplegia. This type depends on position control strategy with a gait pattern, for each joint to walk. The design weights 12 kg but it has actuators only on the knee and hip. The ankle joint is not supported by the device so the user has to use supporters while walking.

To make the lower limb exoskeleton useful and can be used practically, it is important to present a good control strategy. The complex system that consists of the user and the exoskeleton, coupled with the external noise, makes the regular controllers ineffective. This complication makes the researchers work on some much-advanced control systems. Some of them are based on identifying the dynamic parameters of the robot. Other strategies are the adaptive controllers and they are dedicated to general exoskeletons that almost everybody can wear. A good example of these controllers is the adaptive neural methods. The universal approximation of neural networks [7] illustrates an advanced example. On the other hand, neural controllers demand an offline learning to keep away from unacceptable behaviors during the boot phase. Other control techniques that can deal with nonlinear systems is the sliding mode approach [8]. The author [9] track the gait pattern using fuzzy logic controller, although, the results of fuzzy controller led to a recognizable error in the gait pattern performed by the exoskeleton. The author suggests that the error performed by the fuzzy logic controller could be minimized by using an optimal control [10] which suggest an Optimal Control strategy (LQR) to control the lower limb model. This paper presents a newly developed optimal control approach to control the angular position of three joints (hip, knee, and ankle) [10].

Exoskeleton Modeling

The modeling of an exoskeleton robot is considered as the basis of exoskeleton analysis and gait planning, which includes the kinematic modeling and the dynamics modeling. The kinematic modeling can be divided into two sections, the first one is forward kinematics while the second one is the inverse kinematics. Whereas the dynamics modeling is used to calculates the necessary dynamic equations to determine the necessary torques needed to be applied at a certain joint to produce the desired motion [10].

The kinematic modeling

Forward kinematics is also the basics of realizing the visualization of three-dimensional simulation. Denavit-Hartenberg D-H method is the commonly used to define the forward kinematics as the authors in [11] used. The coordinate system for each joint of a single leg of the robot are defined in Figure 3.

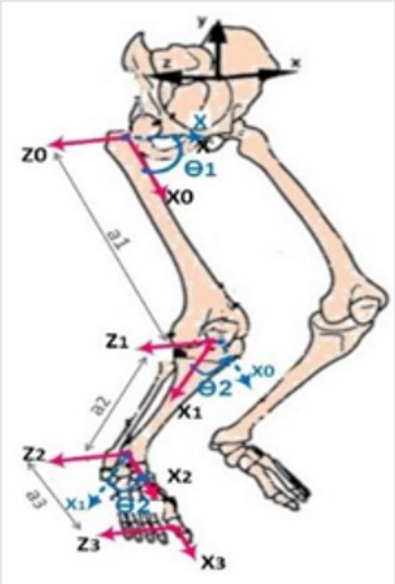

Figure 3: A single leg with relative coordinates for each joint [11].

Note that this leg has only revolute joint, and by applying this convention on the robot leg, we have the following D- H parameters shown in Table 1.

Table 1: D-H Link Parameter.

Link Num.	θi	αi	di	Ai
1	$\theta 1$	0	0	a 1
2	$\theta 2$	0	0	a 2
3	$\theta 3$	0	0	a 3

The calculation process of forward kinematics can be divided into two steps: first calculate the homogeneous transformation matrix between the connected coordinate system, then Kinematical calculation by the chain multiplication of transform matrix. According to the coordinate system established above and using D-H parameters one can define the transformation matrices form joint i to i+1. The general form of transformation matrix is as shown in Equation 1.

$$T_{i+1} = \begin{bmatrix} \cos\theta_i & -\sin\theta_i \cos\alpha_i & \sin\theta_i \sin\alpha_i & a_i\cos\theta_i \\ \sin\theta_i & \cos\theta_i \cos\alpha_i & -\cos\theta_i \sin\alpha_i & a_i\sin\theta_i \\ 0 & \sin\alpha_i & \cos\alpha_i & d_i \\ 0 & 0 & 0 & 1 \end{bmatrix} \quad (1)$$

$$T_{i+1} = \begin{bmatrix} \cos\theta_i & -\sin\theta_i \cos\alpha_i & \sin\theta_i \sin\alpha_i & a_i\cos\theta_i \\ \sin\theta_i & \cos\theta_i \cos\alpha_i & -\cos\theta_i \sin\alpha_i & a_i\sin\theta_i \\ 0 & \sin\alpha_i & \cos\alpha_i & d_i \\ 0 & 0 & 0 & 1 \end{bmatrix} \quad (1)$$

$$J = \begin{bmatrix} -a1s1 - a2s1c2 - a3s1c2+3 & -c1(a2s2 + a3s2+3) & -c1(a3 + s2+3) \\ a1c1 + a2c1c2 + a3c1c2+3 & -s1(a2s2 + a3s2+3) & -s1(a3 + s2+3) \\ s2+3 & c2+3 & a3c2+3 \\ 0 & s_1 & s_1 \\ 0 & -c1 & -c1 \\ 1 & 0 & 1 \end{bmatrix} \quad (5)$$

$$\dot{\theta}(k) = \ddot{\theta}(k)T_s + \theta(k-1) \quad (8)$$

$$\theta(k) = \dot{\theta}(k)T_s + \theta(k-1) \quad (9)$$

$$J = \int_0^\infty (X^T Q X + u^T R u)dt \quad (10)$$

$$u_{ov} = -R^{-1} B^T P_1 X \quad (11)$$

$$ATP + PA - PB_1R^{-1}BTP_1 + Q = 0 \quad (12)$$

By replacing the parameters of the D-H matrix for (i =0, 1, 2), the transformation matrices among the joints can be acquired. The goal of the inverse kinematic is to obtain the angular position of the joints in accordance with the fixed exoskeleton foot coordinate. The equations of the inverse kinematics for each side of the exoskeleton can be written as listed below [10]

$$:\theta = arctan(x)$$

The dynamics modeling

It is important in modeling a robot motion to calculate the robot dynamics so that velocity, acceleration, and forces associated with the robot motion are accounted for. In order to calculate joint torques necessary in robot leg to maintain configuration in response to external forces applied to the foot the Jacobian can be used, and it can be defined as the relationship between joint velocity and manipulator end velocity. The authors in [11] presented the Jacobian Matrix as follows

In order to obtain the dynamic model for the manipulator, one could use the Lagrangian Equation 10 which is specifically suited for determining joint torques for a multi-link manipulator. We use Lagrangian method to calculate the various joint torques necessary in a manipulator to generate desired joint positions, velocities, and accelerations. Those equations provide desired torque called the Euler-Lagrange equations. Where the Lagrangian is the difference between kinetic energy terms K and potential energy P throughout the moving body(s). Depending on the dynamic model in [11], we can simulate the movement of the manipulator as follows (6): K represents Corioles, gravity forces and friction torque. The acceleration equation can be written for each joint as follows (7):

$$\begin{bmatrix} \omega \\ \sigma_1 \\ \varepsilon \\ \omega_2 \\ \alpha_2 \\ \varepsilon_2 \\ \omega_3 \\ \theta_3 \\ \varepsilon \end{bmatrix} = \begin{bmatrix} 1 & 0 & 0 & 0 & 0 & 0 & 0 & 0 & 0 \\ -1 & 0 & 0 & 0 & 0 & 0 & 0 & 0 & 0 \\ 0 & 0 & 0 & 1 & 0 & 0 & 0 & 0 & 0 \\ 0 & 0 & 0 & 0 & 1 & 0 & 0 & 0 & 0 \\ 0 & 0 & 0 & -1 & 0 & 0 & 0 & 0 & 0 \\ 0 & 0 & 0 & 0 & 0 & 0 & 1 & 0 & 0 \\ 0 & 0 & 0 & 0 & 0 & 0 & T_s & 1 & 0 \\ \end{bmatrix} \begin{bmatrix} \omega \\ \sigma_1 \\ \varepsilon \\ \omega_2 \\ \alpha_2 \\ \varepsilon_2 \\ \omega_3 \\ \theta_3 \\ \varepsilon \end{bmatrix} + \begin{bmatrix} M^{-1}T_s & 0 & 0 \\ 0 & M_{21}^{-1}T_s & 0 \\ 0 & M_{22}^{-1}T_s & 0 \\ 0 & 0 & M^{-1}T_s \\ 0 & 0 & M^{-1}T_s \end{bmatrix} \begin{bmatrix} \\ \\ \\ \\ \\ \end{bmatrix} \quad (13)$$

Using Euler first order integration with sample time Ts we have the position and velocity of joints [12] as in Equations 8 & 9:

Equations 7-9 represent the mathematical model of the exoskeleton, which was built in MATLAB/ SIMULINK®, provided Ts in the order of less 1msec.

Symbol	Quantity
θ	Manipulator joint leg
α	link twist
d	link offset
a	link length
$\dot{q}$	vector of joint velocities
J	Jacobian matrix
τ	vector of joint torques

Table II shows the parameters of 4-lower limb leg.

Controller System Design

In these section two types of controllers were described (PID and Optimal Control) and comparison of their responses. First, PID controller was described that's shown in Figure 4. Two PID controllers were designed for each joint: PD for position control and PI for velocity control.

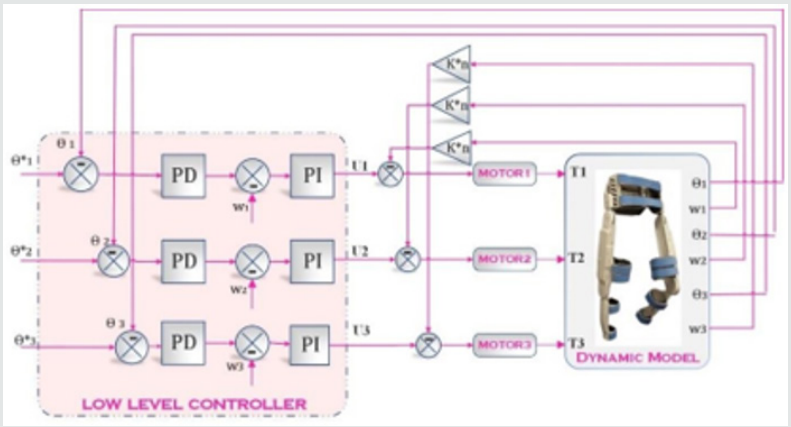

Figure 4: scheme of controller system using PID controller.

The developed control system is shown in Figure 5. The suggested controller is dependent on solving quadratic optimal control problem, has been presented to improve the dynamic performance and correct the position and angular velocity.

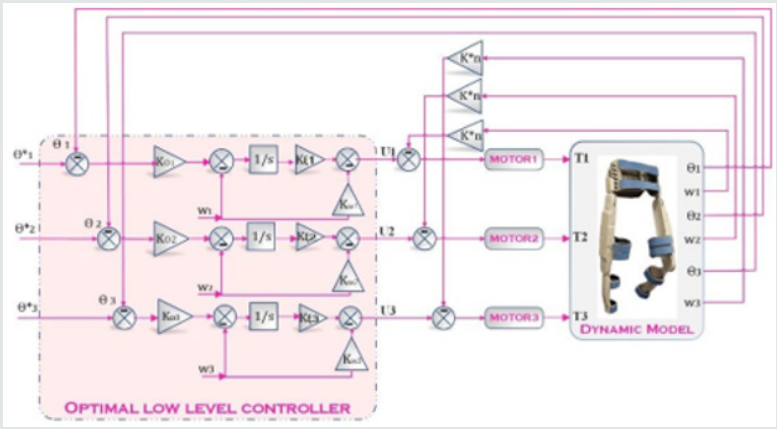

Figure 5: scheme of controller system using LQR controller.

In optimal control, based on Liapunov approach the conditions for stability are formulated first and then the system is designed within these limitations. Thus, the designed system has a configuration with inherent stability characteristics [13].

To solve the quadratic optimal control problem for the system given in (8 and 9), we must determine the control vector u_{op}, which minimizes a selected cost function J as follows (10):

Where:

X_{9x1}: System state vector.

U_{3x1}: Control vector.

Q_{9x9}: Positive semi-definite symmetric matrix determines the relative importance of the error.

R_{3x3}: Positive definite symmetric matrix determines the relative importance of the expenditure of the energy of the control signals.

The optimal control law is given as follows (11):

P_{9x9} is the state covariance matrix which can be obtained from Recite equation which is given as follows (12):

Depending on Equations 8-12 we can derive the extended linear state space equations including optimal controller for the three joints of the exoskeleton as follows (13):

Where:

ω: Joint's angular velocity.

θ: Joint's angular position.

ε: Optimal controller's integral error.

T_s: Sample time.

M: Inertia matrix.

T: Torque acting.

K: The Coriolis effect, centrifugal effect, and the torque applied on joint k by the gravity force.

Table 2: 4-Lower Limb Leg Model Parameters.

Symbol	Quantity
θ	Manipulator joint leg
α	link twist
d	link offset
a	link length
$\dot{q}$	vector of joint velocities
J	Jacobian matrix
τ	vector of joint torques

Table 3: The Error Percentage Average.

Joint	Optimal Controller	PID Controller
Hip	±1.12%	±3.29%
Knee	±1.08%	±2.9%
Ankle	±1.83%	±2.36%

Table 4: Values of the Controller Matrices Q & R, Gains.

Joint	Q & R Matrices	Gains
Hip Joint	85 0 0 $Q1$ = [0 23200], 0 0 18601 R11=0.001	Ko1=507.2 Kw1=304.3 Kξ1=-4066.7
Knee Joint	85 0 0 Q1= [0 2500 0] 0 0 18980 R11=0.001	Ko2=539.4 Kw2=292.7 Kξ2=-4095.2
Ankle Joint	90 0 0 Q1= [0 2500 0] 0 0 18790 R11=0.001	Ko3=542 Kw3=300.2 Kξ3=-4072.2

Simulation Results

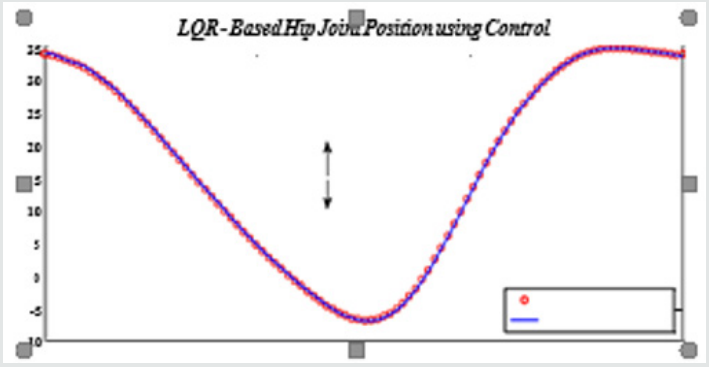

Figure 6:

This section describes the results that obtained with MATLAB/SIMULINK and C code. The objective was to examine the proposed controllers (explained in section IV) and evaluate them in terms of tracking the (Figure 6) desired gait pattern. Figures 7-9 depicts the trajectory stored as a normal gait pattern values and the trajectory performed by the proposed controllers is shown in Figure 4 and Figure 5. Figures 10-12 depicts the torque signal applied on each joint.

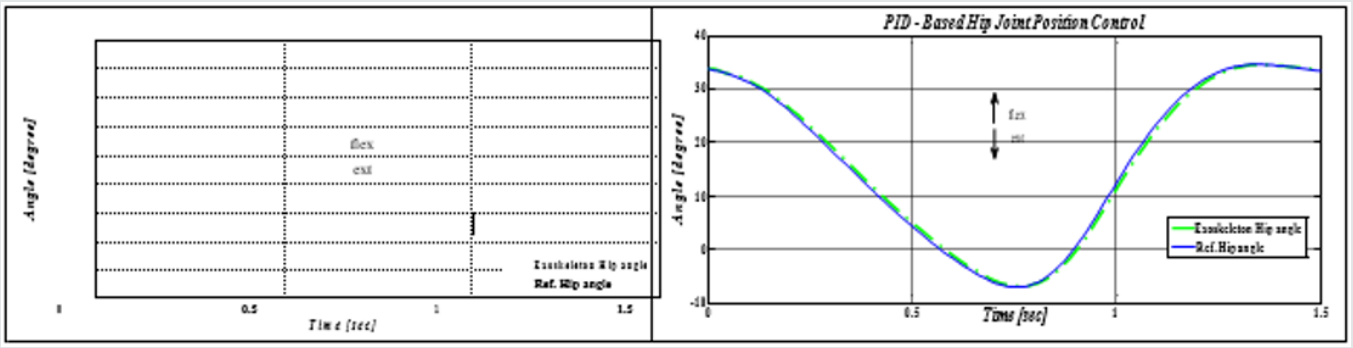

Figure 7: Reference angle & exoskeleton angle of Hip joint using PID & LQR controller

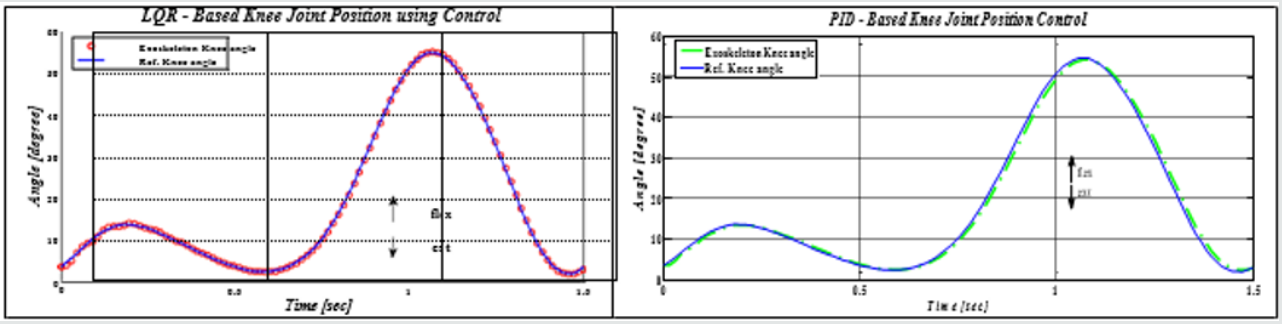

Figure 8: Reference angle & exoskeleton angle of Knee joint using PID & LQR controller.

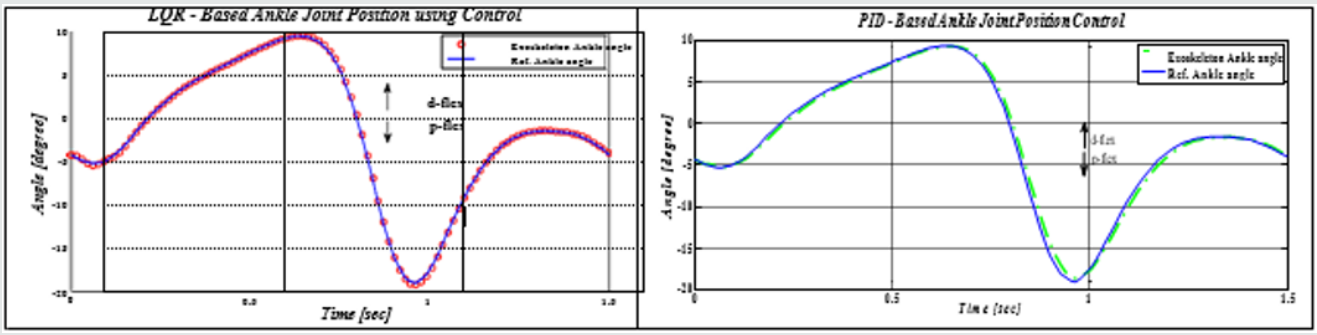

Figure 9: Reference angle & exoskeleton angle of Ankle joint using PID & LQR controller.

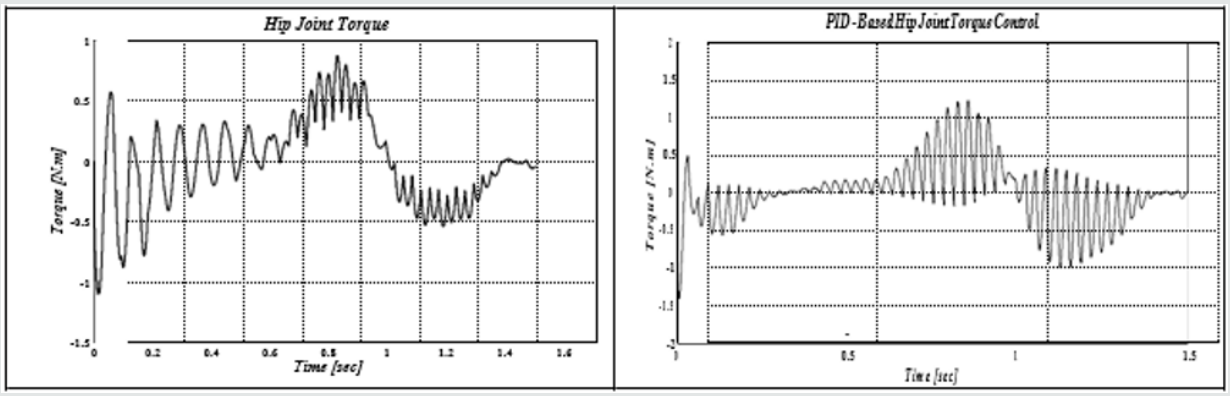

Figure 10: Exoskeleton Hip joint torque Using PID & LQR controller.

As noticed from Figures 7-9 the two controllers have good results regarding the tracking of the gait pattern in each of hip, knee and ankle joints where the error was minimized as good as possible, however when analyzing Figures 10-12, it may be noted that the torque presented by PID controller have a noticeable higher values comparing to the torque values obtained by the LQR controller and that's due to the dynamic coupling among the joints starting from the hip joint to the ankle joint where the PID controller lead to a

higher control law on the actuators, therefore it will practically have a higher power drained from the battery, hence a shorter operation time for the exoskeleton and which is considered as a major factor when designing such applications [14]. Also, it's known that PID gains are challenging to tune specially in real time where different factors can affect the system such as heat and friction, this external effects can dramatically change the parameters of the system therefor will lead to unsatisfied system operation, whereas the LQR controller structure allows to overcome the uncertainly in the system parameters and maintaining of the system high dynamic performance. Table 3 illustrates the error percentage average between the normal gait pattern angles for each joint and the performed values by the two mentioned controllers.

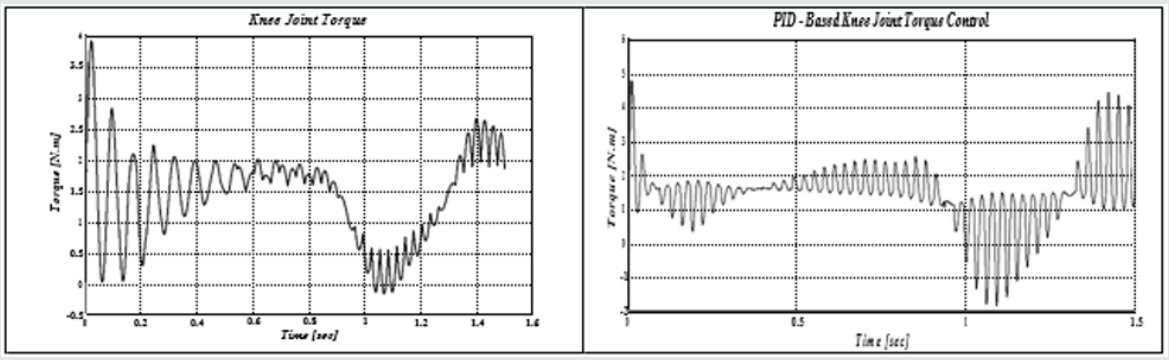

Figure 11: Exoskeleton Knee joint torque Using PID & LQR controller.

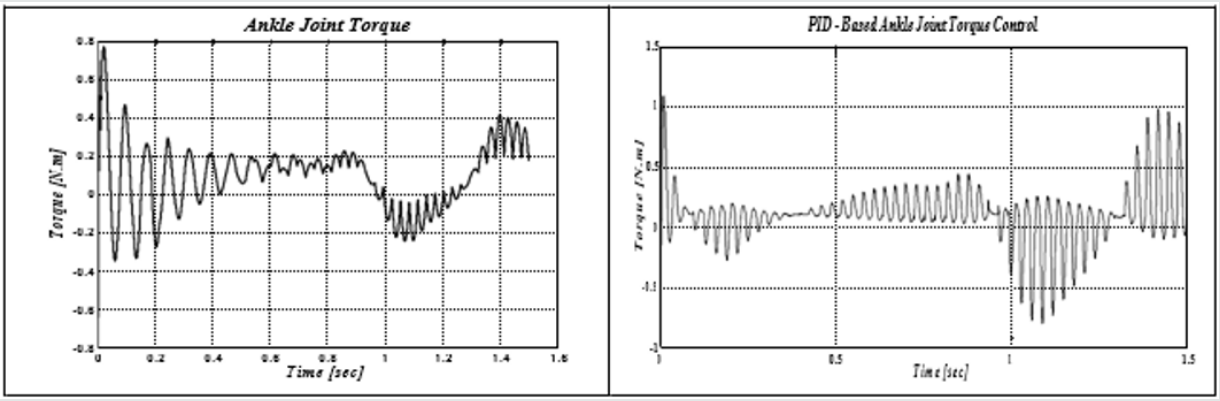

Figure 12: Exoskeleton Ankle joint torque Using PID & LQR controller.

In conclusion, the PID controller provides an acceptable tracking performance regardless the power consumption but it acts poorly with system's parameter mismatch and uncertainty. In the other hand the LQR controller performance is superior to the PID's one with respect to transient and steady state dynamic performance. The inherited inner compensating loops provided with the LQR design help to reject unknown disturbances and enable the controller to be robust against parameters mismatch.

Hardware System Design

Supposedly, the LQR control strategy was implemented on lower limb robotic exoskeleton, but it is not presently existing in our laboratory, so the control strategy is implemented on a humanoid robot instead. The exoskeleton consists of six degrees of freedom, in which the three joints for each side (hip, knee and ankle) are actuated by a BLDC motor. As the exoskeleton joints need more torque and less speed than DC motors can provide directly, a possible solution for increasing torque and reducing the speed is coupling a gearbox to the motor shaft output. This mechanical design contains two different kinds of sensors: kinematic sensors and kinetic sensors. The kinematic sensors measure the angular position, velocity and acceleration, kinetic sensors s used for measuring the force between the exoskeleton and user's limb. Whereas humanoid robot, has a servo motor (Dynamixel AX-12) [15] for hip, knee and ankle joints. The AX-12 servo actuator from Robotics is a smart advanced actuator that involves a gear box, a precision BLDC motor, and it has powerful feedback loop which can read current position of actuator or speed as well as various information such as internal temperature, supply voltage, target position. Besides Dynamixel have unique ID that are controlled by Packet communication on a bus. Regardless of its small size, it can give high torque to produce the necessary power for the model (Figure 13).

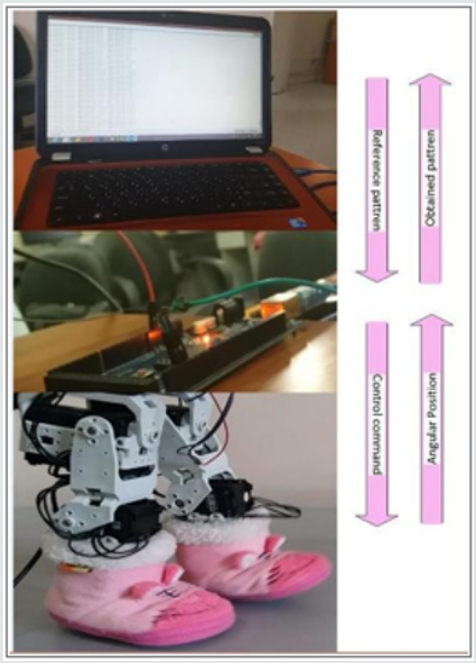

Figure 13:

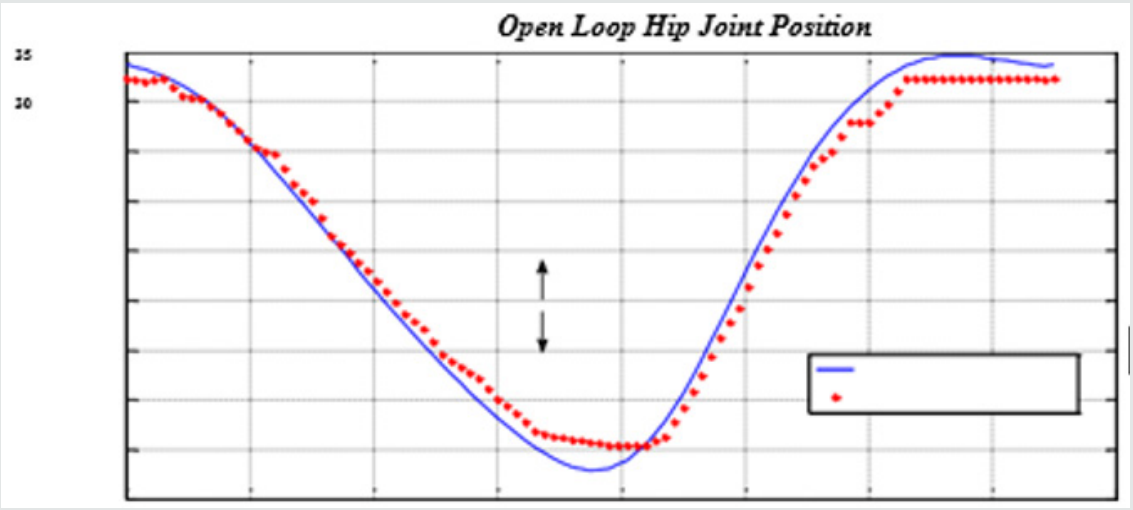

Figure 14: Lab Hardware system design

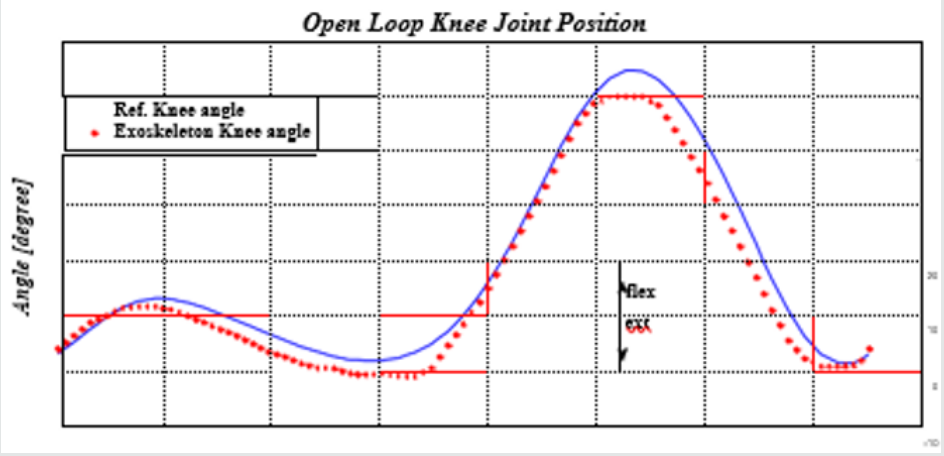

Figure 15: Reference angle & open loop exoskeleton angle of hip joint.

Figures 15-17 illustrate the reference hip, knee and ankle joints angle in sagittal plane (blue) and the hip, knee and ankle actuators angle in sagittal plane performed by the above design (red) in open loop. As noted, the used model weakly tracks the normal gait due to using AX-12 servo actuator in the design. As shown there are remarkable errors specifically in the period [15% to 55%] of gait cycle that includes mid-stance, terminal stance and pre-swing phases, also the period [80% to 95%] which involves mid-swing and terminal swing phases. Through these periods, the body weight is shifted from leg to other, and the trunk is twisted forward, whereas the pelvis is moving towards the stance leg. Addition the motion of joints is opposite (as hip flexes, knee extends). All these effects cause disturbance in the response of the model.

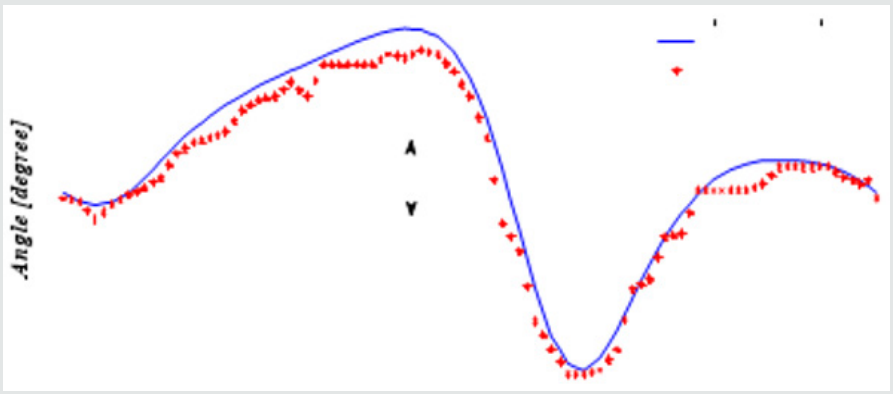

Figure 16: Reference angle & open loop exoskeleton angle of knee joint.

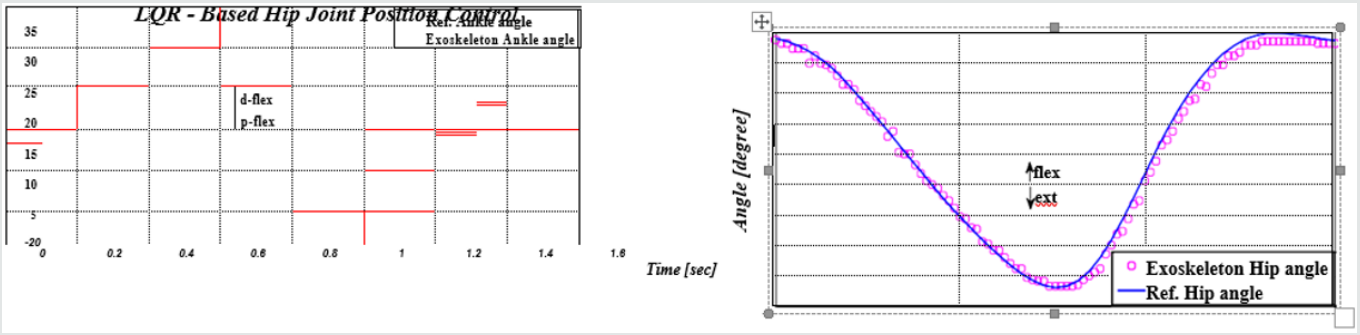

Figure 17: Reference angle & open loop exoskeleton angle of ankle joint.

Results

In this section, we describe the results obtained from humanoid bioloid robot that works as a small- actuated exoskeleton in the open loop then with LQR controller.

Note: The negative gains (Kξ1, Kξ2 and Kξ3) are the integral gains of the optimal controller.

Figures 16-19 show the reference hip, knee and ankle joints angle in sagittal plane (blue) and the hip, knee and ankle actuators angular position in sagittal plane performed by the above design (pink) using optimal controller (LQR). Figure 5 (on page 5) describes the control system of gait cycle. It involves a gait pattern module and three nested control loops, to control the position of hip, knee and ankle joints. Most of the mentioned loops are designed depending on the optimal control approach, considering the interactive dynamic coupling among these control loops due to coupling effect among these joints. Therefore, this system is considered highly nonlinear. This nonlinearity affects the accuracy of the desired trajectory tracking if the controller parameters were not set carefully. As noted from Figures 16-19 the system response is highly improved compared to PID's response, also the gait of the model is too closer to the normal gait of human.

Figure 16 depicts the reference hip joint angle in sagittal plane (blue) and the hip joint angle performed in sagittal plane by the proposed design (pink). It shows the hip joint extends and flexes once along the gait cycle. The maximum attitude for flexion of hip angle (around 34.5°) is reached after the time of Tibia vertical (TV) and before the time of initial contact (IC) (around the mid- swing phase), after that the hip is kept flexed until the first period of the stance phase (IC event). The extension peak is reached in the time of opposite initial contact (before the end of stance phase), after that the hip prepare to flex again. As shown the result of gait tracking motion is corresponding with the desired one.

Figure 18 illustrates the reference knee joint angle in sagittal plane (blue) and the knee joint angle performed in sagittal plane by the proposed design (pink). The knee performs two extension and two flexion peaks per gait cycle. It extends quickly at the end of the swing phase, becoming nearly straight before the time of initial contact (IC), after that starts to flex once again over a period of the loading response and the early part of mid- stance (stance phase knee flexion). The knee joint extends again at the later part of middle of the stance, then begins flexing once again, reaching a peak (around 54.594°) during initial swing (swing phase knee flexion). It

extends again prior to the next initial contact (IC) event. As seen, the described controller LQR design has a perfect performance in tracking the normal gait.

Figure 19 shows the reference ankle joint angle in sagittal plane (blue) and the ankle joint angle performed in sagittal plane by the proposed design (pink). The angular changes of the ankle joint are usually within a few degrees of the neutral position for plantarflexion/dorsiflexion at the initial contact event. After the time of initial contact, the ankle plantar flexes, moving the forefoot down onto the ground. During middle of the stance period, the tibia moves forward along the foot, and the ankle becomes dorsiflexed. From before opposite initial contact until the foot leaves the ground at toe off, the ankle is moving into plantarflexion. During the swing phase, the ankle is moving from a plantarflexed attitude around toe off towards a dorsiflexed attitude in terminal swing until the forefoot has cleared the ground (around feet adjacent). The degree of foot supination reduces following toe off, but the foot remains slightly supinated until the following initial contact.

The presented results in Figures 16-19 proved that the suggested control strategy has been able to decrease the error occurred in the open loop response of the design under investigation, as seen in Figures 15-17. (Figure 20).

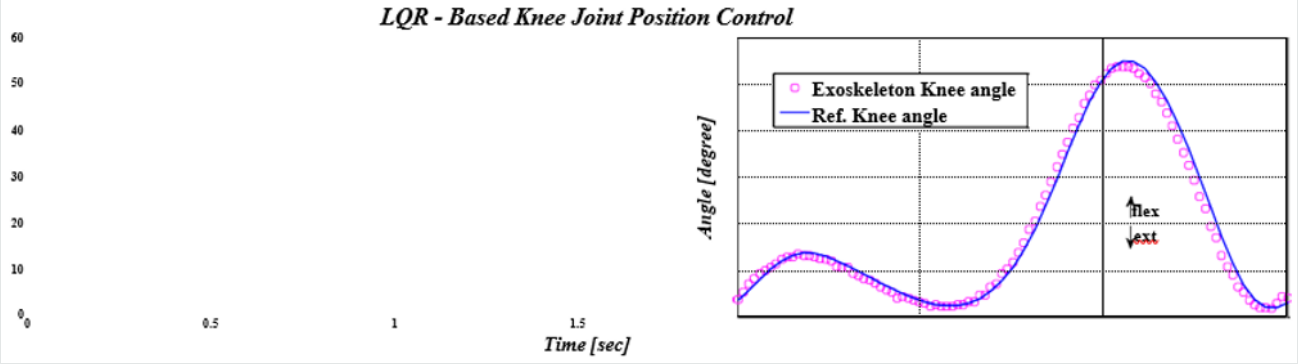

Figure 18: Reference angle & exoskeleton angle of knee joint using controller.

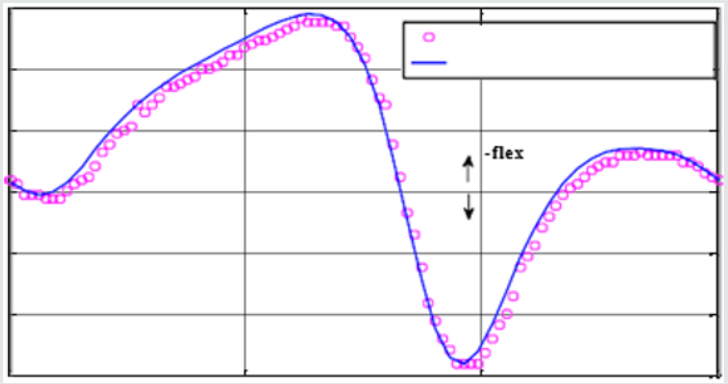

Figure 19: Reference angle & exoskeleton angle of ankle joint using controller.

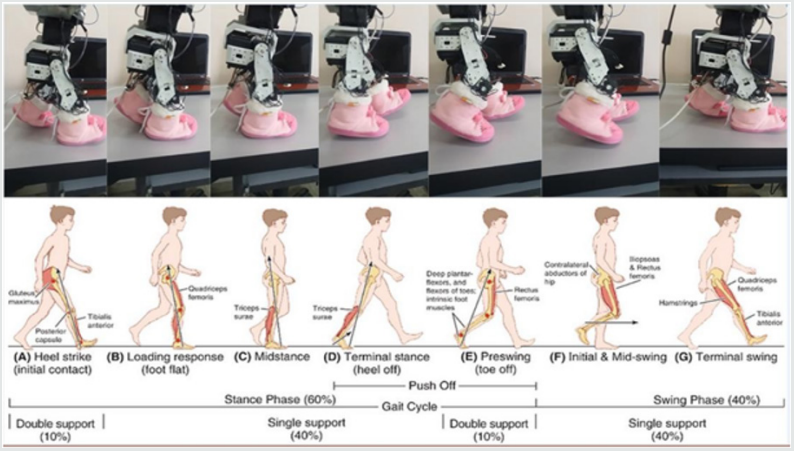

Figure 20: Comparing bioloid steps with normal gait phases.

Conclusion

This work has presented a newly developed a linear quadratic optimal controller (LQR) and is implemented for the Low-Level control, which tracks the angular position of each joint (hip, knee, ankle). It has been illustrated that the proposed control strategy is superior to the conventional control systems that shown in literature. The suggested controller has the ability to cancel the dynamic coupling among the joints starting from the hip joint to the ankle joint. In addition, it can produce a high dynamic to the system. Practical results proved the stability and accuracy of the LQR optimal control approach.

An important matter in being self-supporting is personal motion ability. If you can carry on moving around, you can maintain active and participation in your social life. Powered exoskeletons can help in such situations and, in addition, significantly reduce the burdens on health-care centers, and this was the main goal of the paper.

References

1. Phillips L, Ozer M, Axelson P, Fonseca J (1987) "Spinal cord injury: A guide for patient and family: Raven Press".
2. Magdo Bortole, Jos´e Luis PR, Luis Enrique ML (2013) "Design and Control of a Robotic Exoskeleton for Gait Rehabilitation".
3. Rupal BS, Rafique S, Singla A, Singla E, Isaksson M, et al. (2017) "Lower-limb exoskeletons: Research trends and regulatory guidelines in medical and non-medical applications". International Journal of Advanced Robotic Systems.
4. D´ıaz, I, Gil JJ, S´anchez E (2011) "Lower-limb Robotic Rehabilitation: Literature review and challenges".
5. Neuhaus P, Noorden J, Craig T, Torres T, Kirschbaum J, et al. (2011) "Design and evaluation of mina: A robotic orthosis for paraplegics." IEEE International Conference on Rehabilitation Robotics: [proceedings] 2011: 5975468.
6. Farris R, Quintero H, and Goldfarb M (2012) "Preliminary evaluation of a powered lower limb orthosis to aid walking in paraplegic individuals". Neural Systems and Rehabilitation Engineering IEEE 19: 652-659.
7. Gomes M, Silveira G, Siqueira A (2011) "Gait Pattern Adaptation for an Active Lower-Limb Orthosis Based on Neural Networks". Advanced Robotics 25:1903- 1925.
8. Madani T, Daachi B, Djouani K (2014) "Finite- Time Control of an Actuated Orthosis Using Fast Terminal Sliding Mode". Laboratoire Images, Signaux et Systèmes Intelligents, University of Paris East Créteil, France.
9. Bortole M, Luis Pons Rovira J, Enrique Moreno Lorente L (2013) "Design and Control of a Robotic Exoskeleton for Gait Rehabilation".
10. Hasan Chachati L (2017) "Designing an Electronic System to Control Moving Orthosis Virtual Mechanical System to Emulate Lower Limb". Res J of Aleppo Univ Engineering Sciences Series 135.
11. Hasan Chachati L (2018) "Designing and Implementing an Electronic System to Control Moving Orthosis Virtual Mechanical System to Emulate Lower Limb". Cogent Engineering 5.
12. Kass Hanna D, Joukhadar A (2015) "A Novel Control- Navigation System-Based Adaptive Optimal Controller & EKF Localization of DDMR". International Journal o Advance Research in Artificial Intelligence 4: 29-37.
13. Joukhadar A, Kass Hanna D (2018) "UKF and Adaptive Optimal Control-Based Localization Enhancement of 4WDDMR, ROS Framework-Based Design and Implementation". Cogent Engineering, System and Control Research Article.
14. Burns R (2001) "Advanced Control Engineering". 1st edition, Butterworth-Heinemann, UK.
15. User's Manual "Dynimexal AX-12", 6-2016.

DOI: 10.32474/OAJBEB.2019.03.000171